TMA-VARESE COHORT-1

	TOTAL SAMPLES #50	
GLEASON SCORE	Number	Percentage
≤ 6	16	32%
= 7	17	34%
>7	17	34%
TUMOR STAGE		
≤ T2C	28	56%
T3A-B	21	42%
T3C-T4	1	2%
NODE STATUS		
N0	42	84%
N1	8	16%
PSA (ng/ml) PRE-SURGEY		
≤ 10	32	64%
11 to 20	13	26%
> 20	5	10%

TMA-BERN COHORT-2

	TOTAL SAMPLES #174	
GLEASON SCORE	Number	Percentage
≤ 6	120	69%
= 7	30	17%
>7	24	14%
TUMOR STAGE		
≤ T2C	83	48%
T3A-B	75	43%
T3C-T4	16	9%
NODE STATUS		
N0	173	99%
N1	1	1%
N2	0	0%
PSA (ng/ml) PRE-SURGEY		
≤ 10	64	37%
11 to 20	60	34%
> 20	50	29%

Supplementary Figure 1
Histopathological and clinical parameters of primary prostate cancer patients in the two patient cohorts evaluated by TMAs.

Supplementary Figure 2

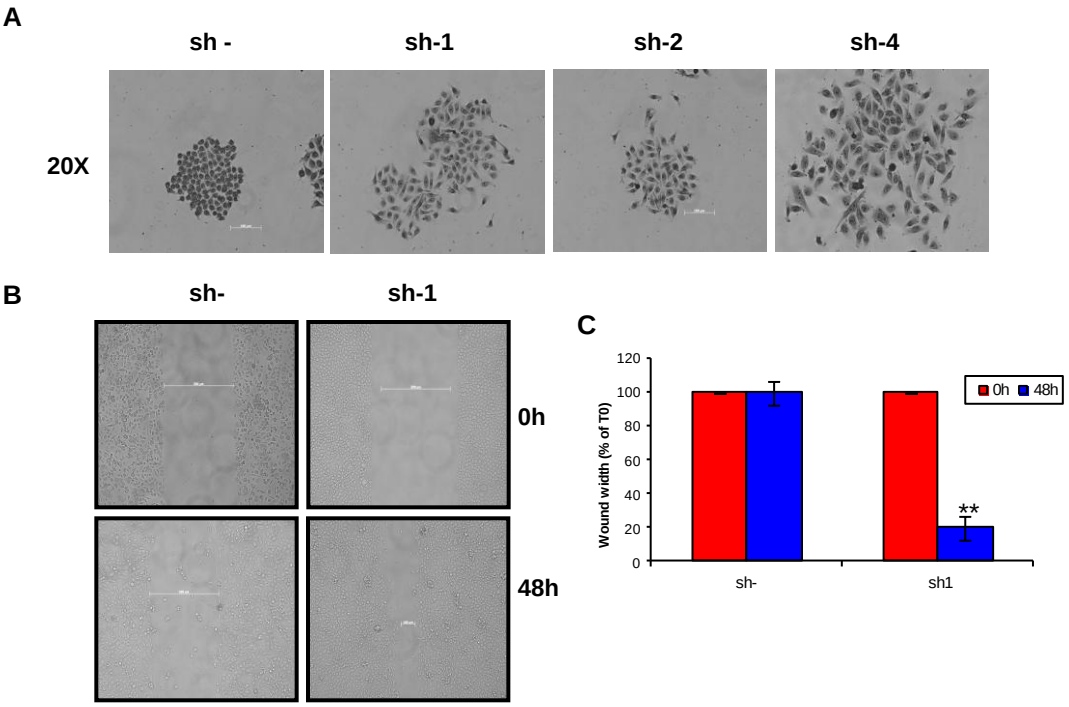

Supplementary Figure 2

ESE3/EHF knockdown induces epithelial to mesenchymal transition. (A) Morphological changes induced by stable ESE3 knockdown by shRNA in RWPE-1 cells evaluated by phase-contrast microscopy. (B) Increased cell migration in ESE3^{kd}- RWPE-1 (sh1) cells compared to RWPE-1 control (sh-) cells in scratch-wound healing assay. (C) Wound width as percentage at time 0 from triplicate experiments. **P<0.01.

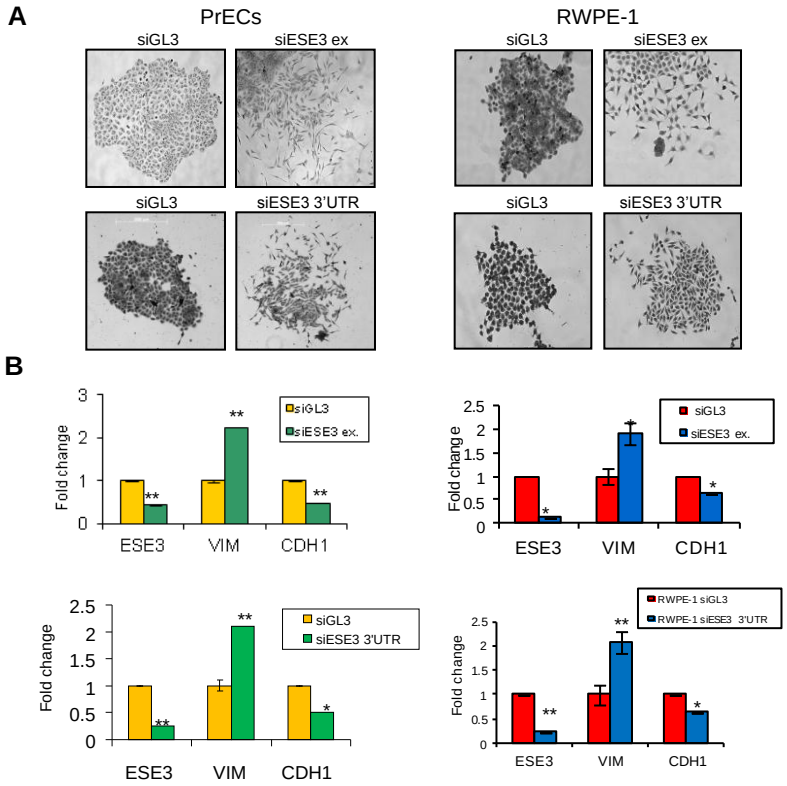

Supplementary Figure 3

Transient downregulation of ESE3/EHF induces a mesenchymal phenotype. (A) Morphological changes induced by transient ESE3 knockdown with ESE3 targeting siRNAs (siESE3ex and siESE3 3'UTR) in PrECs and RWPE-1 cells evaluated by phase-contrast microscopy. (B) ESE3, Vimentin (VIM) and CDH1 RNA level following transient ESE3 knockdown in PrECs and RWPE-1 cells evaluated by QRT-PCR. P values were determined using *t-test.* *P<0.05; **, P<0.01.

Supplementary Figure 4

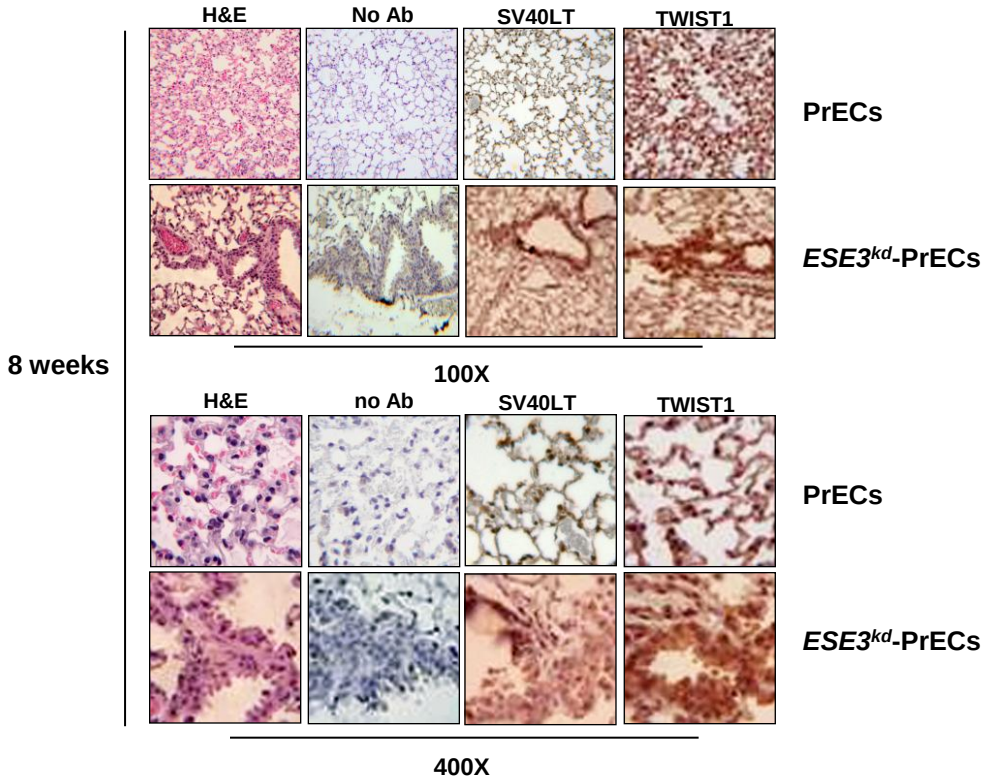

Supplementary Figure 4

In vivo formation of lung metastasis. Control and ESE3^{kd}-PrECs cells were inoculated by tail vein injection into immunodeficient mice (n=4/group). Mice were sacrificed at 8 weeks to perform histological analysis of multiple lung sections following H&E staining and immunostaining for SV40 large T antigen. Representative sections of the lungs of mice injected with control and ESE3^{kd}-PrECs cells and examined after 8 weeks are shown.

Supplementary Figure 5

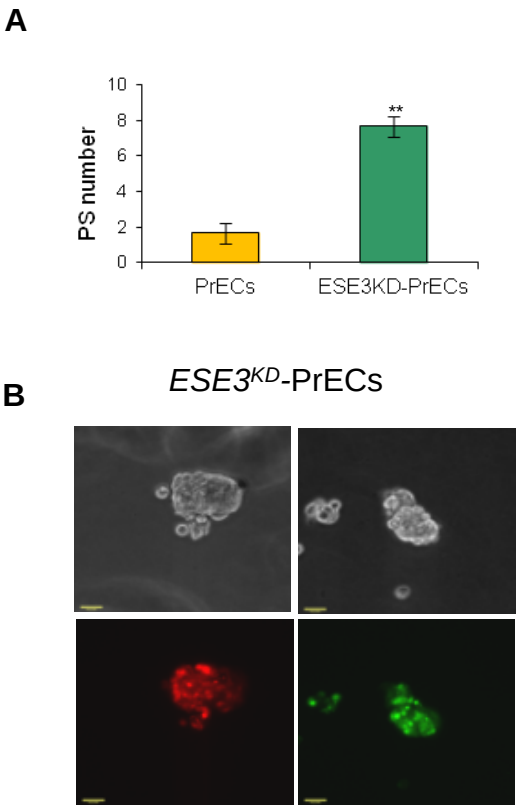

Supplementary Figure 5

Prostato-sphere formation by prostate epithelial cells. (A) Sphere-forming assay under limiting dilution conditions. Cells were plated in 96-well plates and prostato-spheres were counted after 7-10 days. (B) Phase-contrast (upper panels) and fluorescence microscopy (lower panels) images of prostato-spheres of ESE3^{kd}-PrECs. Cells were stained separately with either a green or red fluorescent dye and then mixed prior to the sphere-forming assay. **, P<0.01.

Supplementary Figure 6

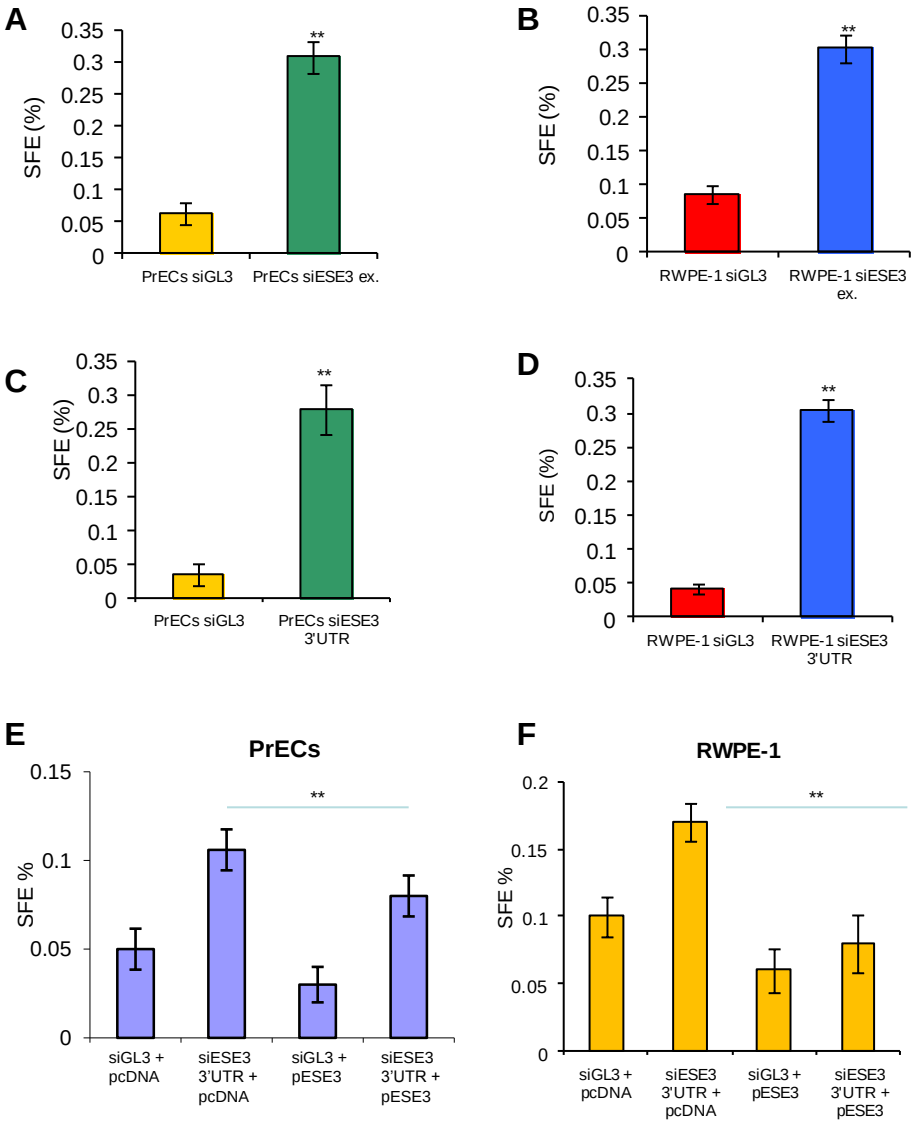

Supplementary Figure 6

Transient downregulation of ESE3/EHF in PrECs and RWPE-1 cells induces stem-like properties. (A-B) Prostato-sphere formation following transient ESE3/EHF knockdown with siRNA targeting exon 2, siESE3ex, in PrECs and RWPE-1 cells. (C-D) Prostato-sphere formation following transient ESE3/EHF knockdown with the siRNAs targeting the 3'UTR. (E-F) Prostato-sphere assay after ESE3/EHF knockdown with 3'UTR siRNAs and concomitant transfection of an ESE3/EHF expression vector or control pcDNA in PrECs and RWPE-1. **, P<0.01.

Supplementary Figure 7

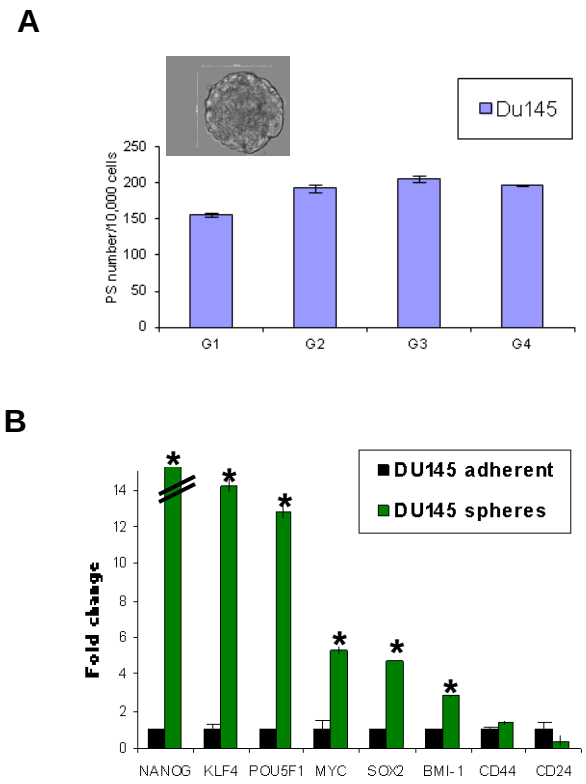

Supplementary Figure 7

Prostato-sphere formation and stem-like properties in DU145 cells. (A) In vitro sphere-forming and self-renewal of DU145 cells. (B) Expression of cancer stem cell genes in adherent cells and prostato-spheres of DU145 cells determined by QRT-PCR. P values were determined using t-test. *P<0.05; **, P<0.01.

Supplementary Figure 8

Survival analysis

ESE3 STAIN	N total	N. events	Troncated	%
Score = 0-1(weak/Neg)	156	48	108	69.2%
Score = 2 (Normal-like)	18	1	17	94.4%
Global	174	49	125	71.8%

Biochemical relapse analysis

ESE3 STAIN	N total	N. events	Troncated	%
Score = 0-1(weak/Neg)	153	119	34	22.2%
Score = 2 (Normal-like)	18	10	8	44.4%
Global	171	129	42	24.6%

Gleason score distribution

GLEASON SCORE	TOTAL %	ESE3 score weak/Neg	ESE3 score Normal-like
≤6	69%	106 (68%)	13 (72%)
7	17%	27 (18%)	2 (11%)
≥8	14%	22 (14%)	3 (17%)

Supplementary Figure 8
Overall survival and PSA biochemical relapse in prostate cancer patients. Tables show the data relative to the patients included in the analysis described in Figure 8. Gleason score distribution was not statistically different between the two groups.